

Real-Time Spatial Estimates of Snow-Water Equivalent (SWE)

Sierra Nevada Mountains, California

April 13, 2018

Team: Noah Molotch^{1,2}, Leanne Lestak¹, Dominik Schneider¹, and Keith Musselman¹

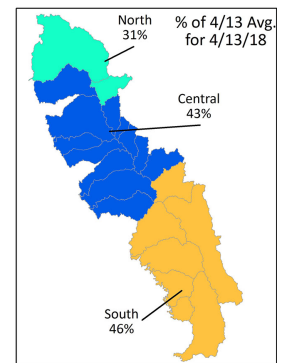
¹ Center for Water Earth Science & Technology, Institute of Arctic and Alpine Research, Uni of Colorado Boulder

² Jet Propulsion Laboratory, California Institute of Technology

Contact: Leanne.Lestak@colorado.edu

Summary of current conditions

The map on the right shows mean spatial SWE above 5000' for 3 regions in the Sierra Nevada and corresponds to a daily map released by the CA DWR, which uses snow sensor data. Unlike the CA DWR map this map only includes the Feather and the Truckee in the North region. Snow levels have increased in elevation since the last report and snow depths have decreased at higher elevations. A number of snow sensors are recording 0 SWE in the south which will effect the regression estimates. The modeled conditions could be sensitive to the regression algorithm and data input and availability. Please be sure to read the *Data Issues / Caveats* section for a discussion of persistent challenges or flagged uncertainties of the SWE product.



About this report

This is an experimental research product that provides near-real-time estimates of snow-water equivalent (SWE) at a spatial resolution of 500 m for the Sierra Nevada in California from mid-winter through the melt season. The report is released within a week of the date of data acquisition at the top of the report. A similar report covering the Intermountain West, makes its debut this season and will be distributed to water managers in Colorado, Utah and Wyoming.

The spatial SWE analysis method for the Sierra Nevada uses the following data as inputs:

- In-situ SWE from all operational CA snow gage sensor sites
- MODSCAG fractional snow-covered area (fSCA) data from recent cloud-free MODIS satellite images
- Physiographic information (elevation, latitude, upwind mountain barriers, slope, etc.)
- Historical daily SWE patterns (2000-2014) retrospectively generated using historical MODSCAG data and an energy-balance model that back-calculates SWE given the fSCA time-series and meltout date for each pixel

For more details on the estimation method see the *Methods* section below. Please be sure to read the *Data Issues / Caveats* section for a discussion of persistent challenges or flagged uncertainties of the SWE product.

Data availability for this report

90 snow gage sites in the Sierra Nevada network were recording SWE values out of a total of 114 sites; 9 were reporting but had zero SWE (shown in yellow in Figure 3, left map); and 15 were offline (shown in red in Figure 3, left map).

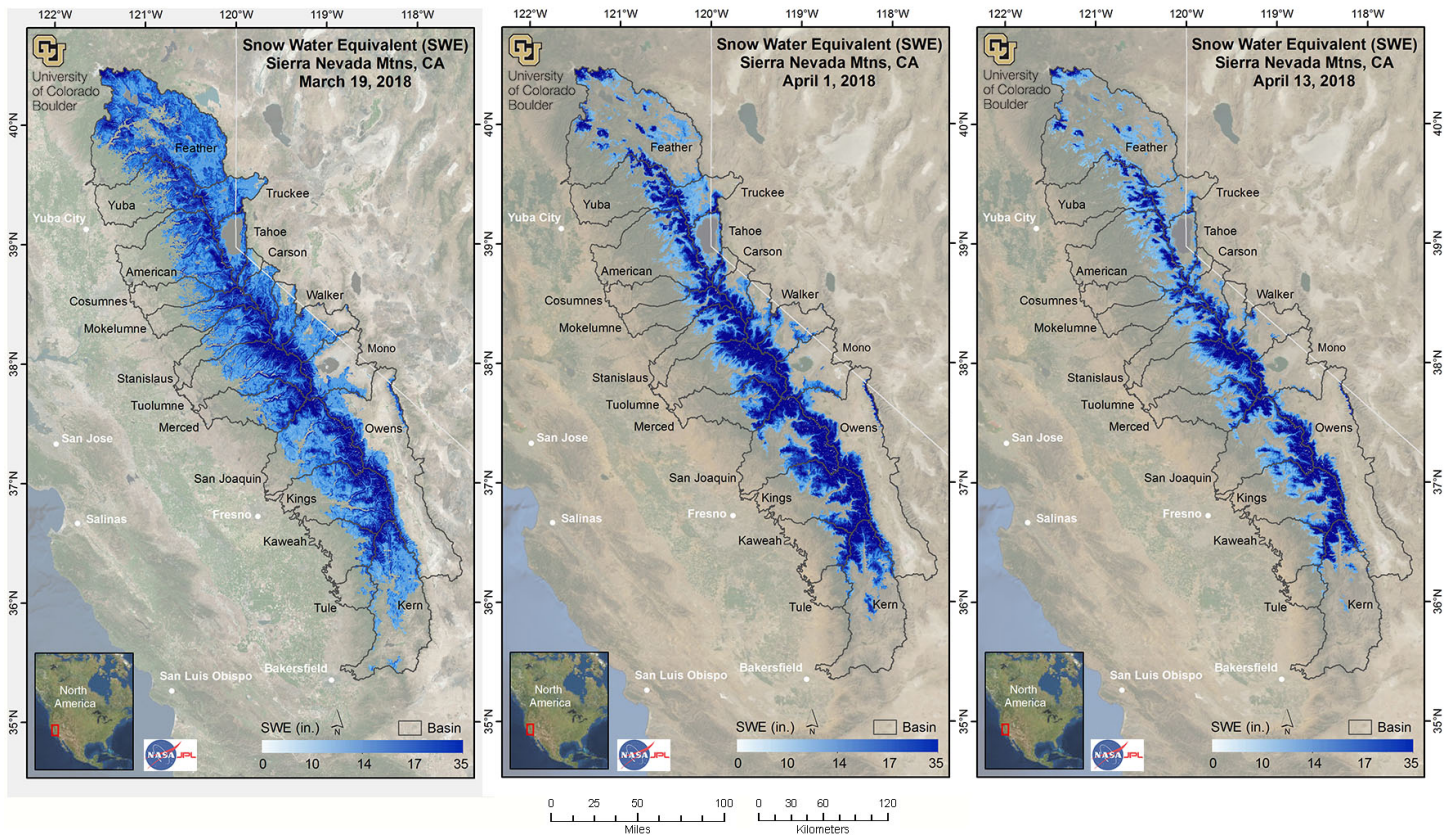


Figure 1. Estimated SWE across the Sierra Nevada. SWE amounts for March 19, 2018 (left), April 1st (middle), and April 13th (right).

The value of spatially explicit estimates of SWE

Snowmelt makes up the large majority (~60-85%) of the annual streamflow in the Sierra Nevada. The spatial distribution of snow-water equivalent (SWE) across the landscape is complex. While broad aspects of this spatial pattern (e.g., more SWE at higher elevations and on north-facing exposures) are fairly consistent, the details vary a lot from year to year, influencing the magnitude and timing of snowmelt-driven runoff.

SWE is operationally monitored at just over a hundred snow gage sensor sites spread across the Sierra Nevada, providing a critical first-order snapshot of conditions, and the basis for runoff forecasts from the CA DWR, NRCS, and NOAA. However, conditions at snow sensor sites (e.g., percent of normal SWE) may not be representative of conditions in the large areas between these point measurements, and at elevations above and below the range of the sensor sites. The spatial snow analysis creates a detailed picture of the spatial pattern of SWE using snow sensors, satellite, and other data, extending beyond the snow sensor sites to unmonitored areas.

Interpreting the spatial SWE estimates in the context of SNOTEL

The spatial product estimates SWE for every pixel where the MODSCAG product identifies snow-cover. Comparatively, snow sensor samples 8-20 points per basin within a narrower elevation range. Thus, the basin-wide percent of average from the spatial SWE estimates is not directly comparable with the snow sensor basin-wide percent of average. A better comparison might be made with the % average in the elevation bands (Table 2) that contain snow sensor sites.

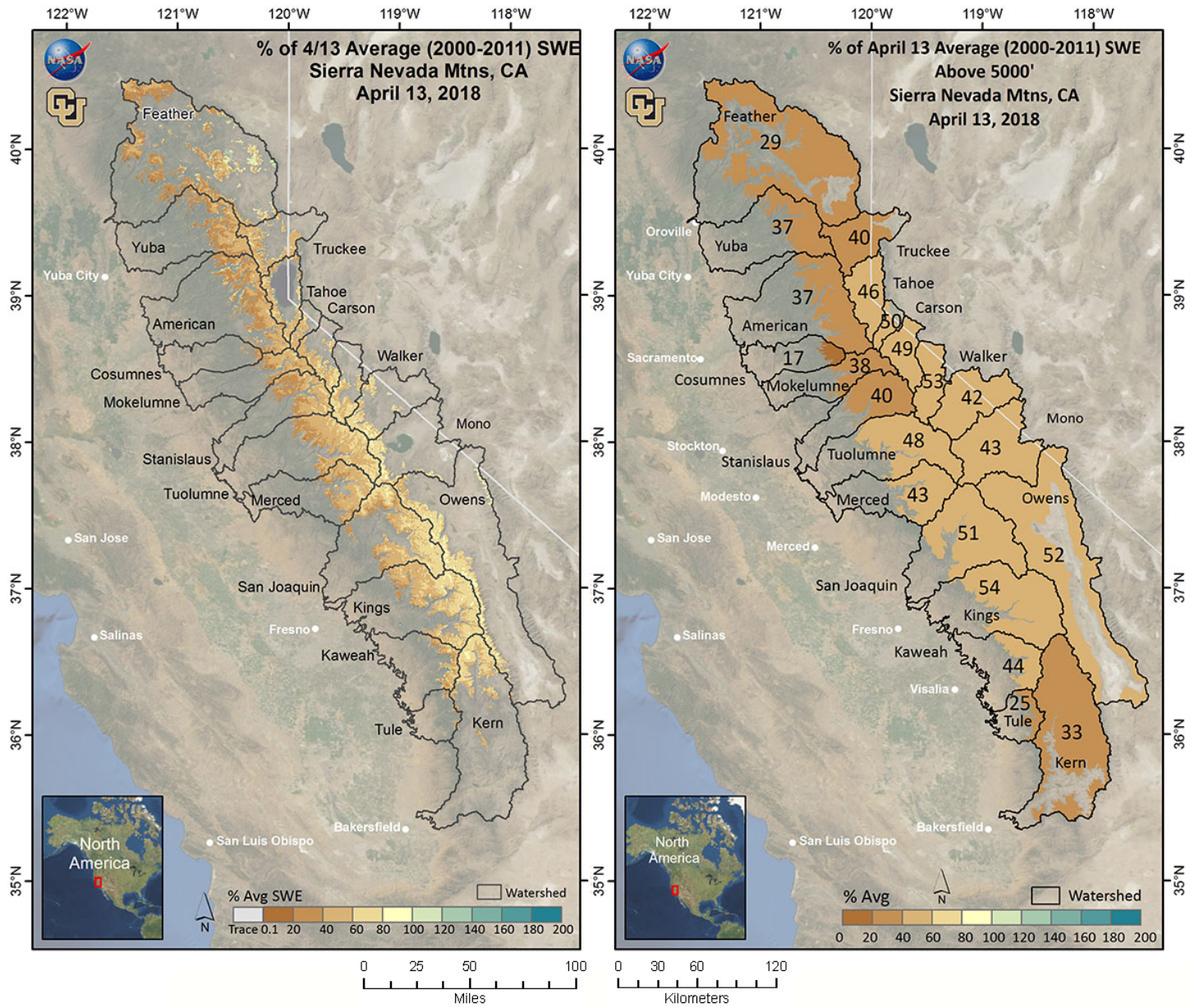


Figure 2. Estimated % of average SWE across the Sierra Nevada, April 13, 2018. Percent of average (2000-2011) SWE for April 13, 2018 for the Sierra Nevada, calculated for each pixel (left) and basin-wide (right). Basin-wide percent of average is calculated across all model pixels >5000' elevation.

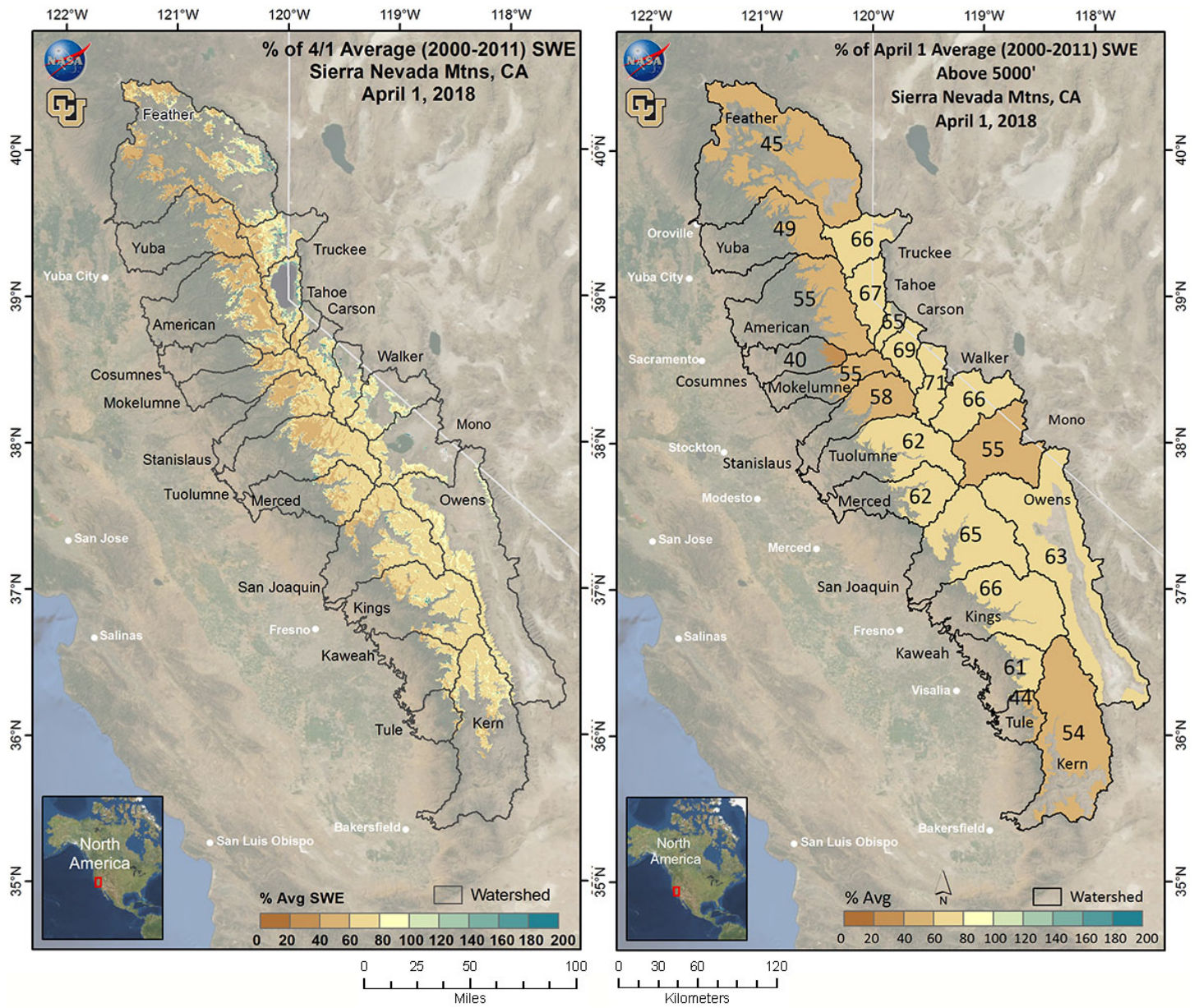


Figure 3. Estimated % of average SWE across the Sierra Nevada. Percent of average (2000-2011) SWE for April 1, 2018 for the Sierra Nevada, calculated for each pixel (left) and basin-wide (right). Basin-wide percent of average is calculated across all model pixels >5000' elevation.

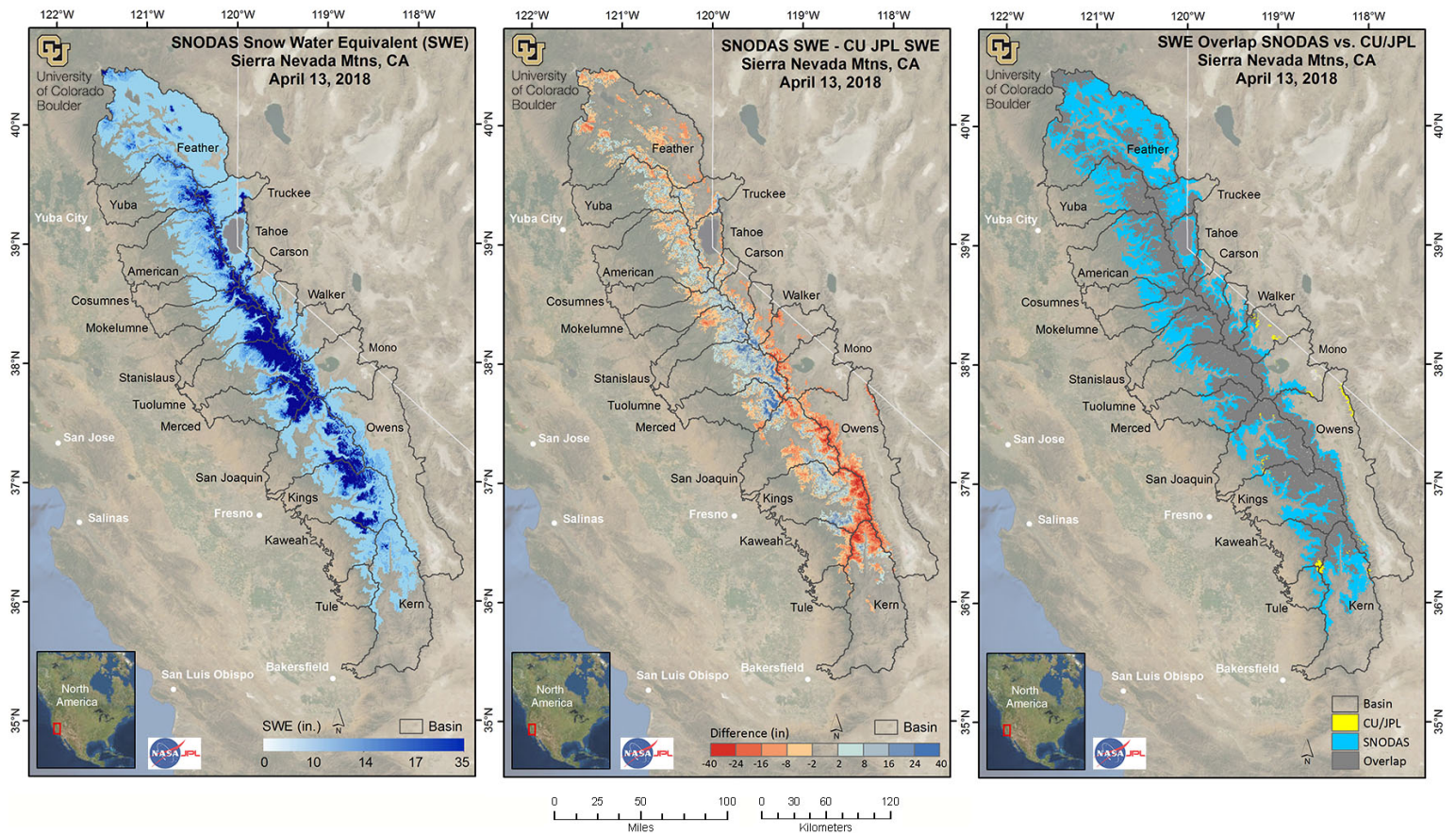


Figure 4. Comparison of CU/JPL regression SWE product and SNODAS SWE for the Sierra Nevada. The map on the left shows estimated SWE for April 13th from the NOAA National Weather Service's National Operational Hydrologic Remote Sensing Center (NOHRSC) SNOW Data Assimilation System (SNODAS). The middle map shows the difference between the April 13th SNODAS SWE estimate and CU/JPL regression SWE estimate. Red pixels denote areas where SNODAS SWE is less than CU/JPL SWE and blue pixels show areas where SNODAS SWE is higher than CU/JPL SWE. The map on the right shows the snow-cover extent of SNODAS and CU/JPL SWE estimates. Yellow pixels show where the location of CU/JPL snow extends beyond the location of the SNODAS snow extent. Blue pixels show where the SNODAS snow extends beyond the CU/JPL snow extent. Gray areas indicate regions where both products agree on the snow-cover extent.

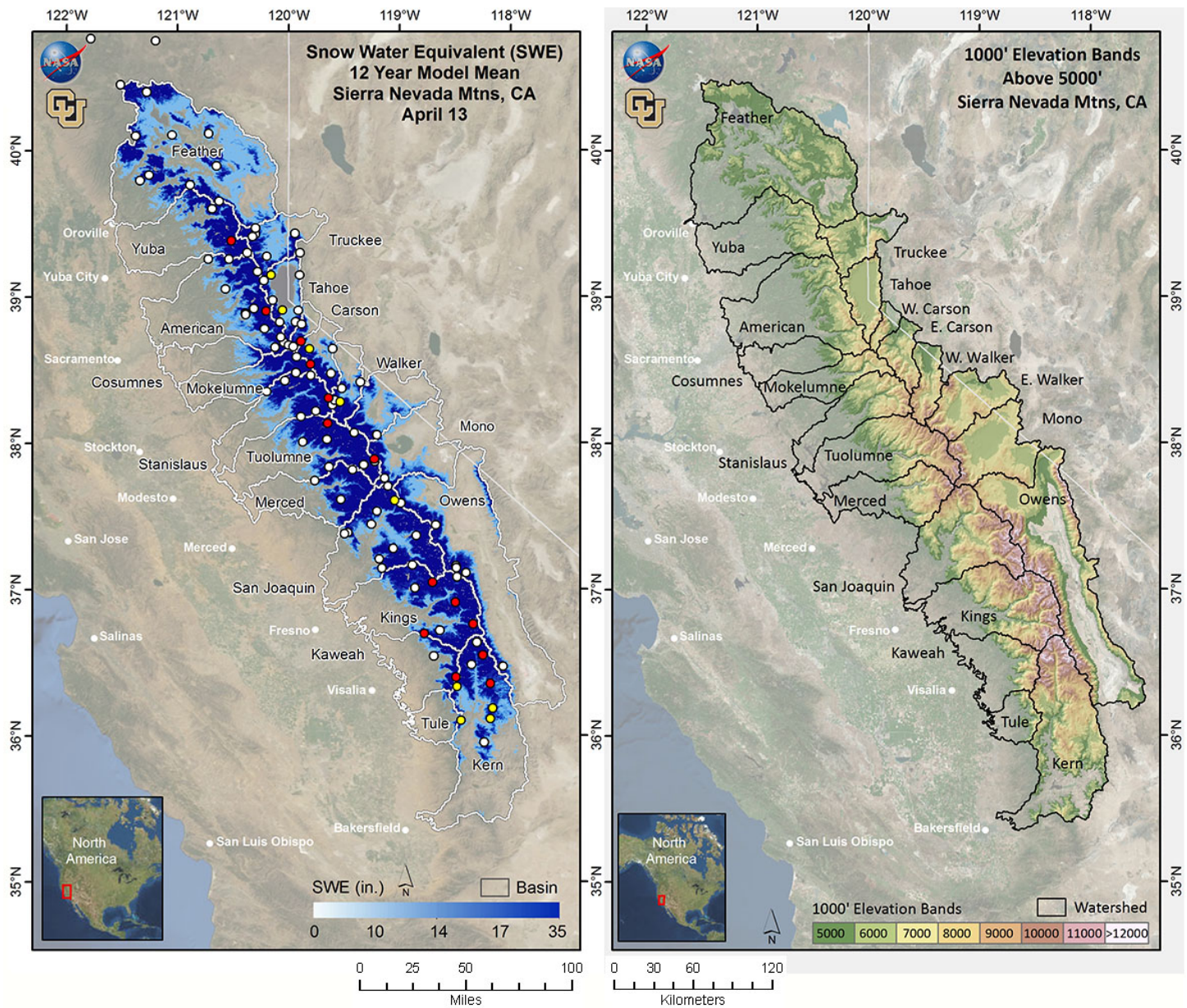


Figure 5. Mean SWE and Elevation Bands for the Sierra Nevada. Mean SWE (2000-2011) amounts for April 13th (left), and Banded Elevation map identifies basins used in this report (black boundaries) and 1000' elevation bands (colored shading) that match those used in Table 1 and Table 2. Map on left shows snow gage sensor sites recording SWE on April 13, 2018 (white), sites that were offline are shown in red and sites recording zero SWE are shown in yellow.

Methods

The spatial SWE estimation method is described in Schneider and Molotch (2016). The method uses linear regression in which the dependent variable is derived from the operationally measured in situ SWE from all online snow sensor sites in the domain. The snow sensor SWE observations are scaled by the fractional snow-covered area (fSCA) across the 500 m pixel containing that snow sensor site before being used in the linear regression model. The fSCA is a near-real-time cloud-free MODIS satellite image which has been processed using the MODIS Snow Cover and Grain size (MODSCAG) fractional snow-covered area algorithm program (Painter, et. al. 2009, snow.jpl.nasa.gov).

The following independent variables (predictors) enter into the linear regression model:

- Physiographic variables that affect snow accumulation, melt, and redistribution, including elevation, latitude, upwind mountain barriers, slope, and others. See Figure 2 in Schneider and Molotch (2016) for the full set of these variables.
- The historical daily SWE pattern (2000-2014) retrospectively generated using historical MODSCAG data, and an energy-balance model that back-calculates SWE given the fractional Snow-Covered Area (fSCA) time series and meltout date for each pixel. See Guan, et. al., 2013 for details. (For computational efficiency, only one image from either the 1st or 15th of aa

month during the 2000-2014 period that best matches the real-time SNOTEL-observed pattern is selected as an independent variable.)

The real-time regression model for this date has been validated by cross-validation, whereby 10% of the SNOTEL data are randomly removed and the model prediction is compared to the measured value at the removed SNOTEL stations. This is repeated 30 times to obtain an average R-squared value, which denotes how closely the model fits the SNOTEL data. During development of this regression method, the model was also validated against independent historical SWE data collected in snow surveys at 9 locations in Colorado, and an intensive field survey in north-central Colorado.

Data Issues/Caveats – IMPORTANT - READ THIS!

- There are occasionally problems with lower-elevation SWE estimates due to recent snowfall events that result in extensive snow-cover extending to valley locations where measurements are not available. This scenario results in an over-estimation of lower- elevation SWE.
- A known limitation of the model occurs late in the melt season when snow at the SNOTEL sites melts out, but snow remains at higher elevations. In this case, the model tends to underestimate SWE at these under-monitored upper elevations. Thus, late-season SWE prediction at higher elevations may be less accurate than earlier in the snow season.
- Cloud cover can obscure satellite measurements of snow-cover. While careful checks are made, occasionally the misclassification of clouds as snow or *vice versa* may result in the mischaracterization of SWE or bare-ground.
- Although data QA/QC is performed, occasional SNOTEL sensor malfunction may result in localized SWE errors.
- Anomalous snow years or snow distributions may cause SWE error due to the model design to search for similar SWE distributions from previous years. If no close seasonal analogue exists, the model is forced to find the most similar year, which may result in error.
- Dense forest cover at lower elevations where snow-cover is discontinuous can cause the satellite to underestimate the snow-cover extent, leading to underestimation of SWE.

Table 1. Estimated SWE by basin. The basin-wide SWE values and averages, are across all pixels at elevations >5000'. Shown are April 1st percent of April 1st average and April 13th percent of April 13th average SWE (between 2000-2011, April 1st and April 13th mean SWE, and the difference between April 1st and April 13th SWE summarized for each basin. The last column shows April 13th mean SWE from SNODAS*.

Basin	4/1/18 % 4/1 Avg.	4/13/18 % 4/13 Avg.	4/1/18 SWE (in)	4/13/18 SWE (in)	4/1 thru 4/13/18 Chg. in SWE (in)	Area (mi ²) > 5000'	4/13/18 SNODAS* (in)
American	55	37	12.7	8.7	-4.1	798.0	8.9
Cosumnes	40	17	5.2	2.4	-2.8	87.8	1.0
E Carson	69	49	10.6	7.1	-3.6	400.2	6.4
E Walker	66	42	6.2	3.5	-2.7	801.4	1.5
Feather	45	29	6.5	4.2	-2.3	2,086.3	2.5
Kaweah	61	44	9.6	6.3	-3.3	315.9	3.6
Kern	54	33	6.2	3.4	-2.8	1,770.6	1.0
Kings	66	54	14.8	11.3	-3.5	1,220.0	8.4
Merced	62	43	13.7	9.2	-4.4	535.7	12.1
Mokelumne	55	38	13.4	9.2	-4.2	316.3	10.4
Mono	55	43	4.5	3.0	-1.5	1,088.0	1.6
Owens	63	52	5.5	4.1	-1.4	2,167.6	1.1
San Joaquin	65	51	15.0	11.1	-3.9	1,226.8	7.9
Stanislaus	58	40	14.2	9.7	-4.6	558.0	11.9
Tahoe	67	46	13.1	8.8	-4.3	509.8	8.6
Truckee	66	40	10.2	5.8	-4.3	556.2	5.6
Tule	44	25	3.0	1.4	-1.6	138.2	0.2
Tuolumne	62	48	15.4	11.8	-3.7	908.9	16.0
W Carson	65	50	10.9	8.1	-2.7	123.9	8.0
W Walker	71	53	9.9	7.0	-2.9	432.7	6.9
Yuba	49	37	13.1	9.9	-3.2	518.9	9.4

* This is a comparison to the SNODAS (SNOW Data Assimilation System) nationwide product from the National Weather Service.

Table 2. Estimated SWE by basin and elevation band. Elevation bands begin at 5000' and extend past the highest point in the basin. Note that the area of the highest 2-5 bands is typically much smaller than the lower bands. Shown are April 1st percent of April 1st average and April 13th percent of April 13th average SWE (between 2000-2011), April 1st and April 13th mean SWE, and the difference between April 1st and April 13th SWE summarized for each 1000' elevation band inside each basin. The last column shows April 13th mean SWE from SNODAS*.

Basin	Elevation Band	4/1/18 % 4/1 Avg.	4/13/18 % 4/13 Avg.	4/1/18 SWE (in)	4/13/18 SWE (in)	4/1 thru 4/13/18 Chg. in SWE (in)	Area Sq Mi	4/13/18 SNODAS* (in)
American	5000-6000'	49	21	6.1	2.7	-3.4	295.5	3.5
	6000-7000'	52	33	12.6	8.1	-4.5	261.0	7.4
	7000-8000'	57	45	19.0	14.9	-4.2	166.3	13.6
	8000-9000'	63	52	24.6	19.7	-4.9	67.8	24.5
	9000-10,000'	65	54	29.5	24.0	-5.5	8.6	32.5
Cosumnes	5000-6000'	23	7	2.1	0.7	-1.4	57.9	0.5
	6000-7000'	54	20	10.1	4.0	-6.1	22.9	1.4
	7000-8000'	52	40	15.5	12.2	-3.3	6.4	3.7
E. Carson	5000-6000'	2	0	0.0	0.0	0.0	65.9	0.0
	6000-7000'	57	4	3.2	0.2	-3.1	90.7	0.1
	7000-8000'	73	36	11.7	5.4	-6.4	104.8	3.0
	8000-9000'	68	57	17.7	14.3	-3.4	95.2	11.5
	9000-10,000'	73	62	22.3	18.7	-3.6	33.8	23.4
	10,000-11,000'	76	66	24.8	21.4	-3.5	10.3	30.7
	> 11,000'	72	67	27.5	25.5	-2.1	0.3	24.6
E. Walker	5000-6000'	6	0	0.0	0.0	0.0	21.5	0.0
	6000-7000'	36	0	0.1	0.0	-0.1	211.7	0.0
	7000-8000'	74	5	2.1	0.2	-1.9	254.4	0.0
	8000-9000'	76	25	9.9	3.0	-6.9	185.8	0.7
	9000-10,000'	75	62	17.4	13.5	-3.9	76.6	6.5
	10,000-11,000'	76	70	23.8	22.1	-1.7	40.6	11.6
	11,000-12,000'	76	73	25.6	24.5	-1.1	10.3	7.3
> 12,000'	31	78	26.9	27.8	0.9	0.3	7.3	
Feather	5000-6000'	55	17	3.3	1.9	-1.4	1,259.3	1.4
	6000-7000'	61	36	10.2	6.7	-3.6	706.5	3.3
	7000-8000'	67	50	17.1	13.8	-3.3	114.3	8.8
	8000-9000'	0	54	23.9	18.9	-5.0	3.7	19.8
Kaweah	5000-6000'	14	0	0.0	0.0	0.0	62.1	0.2
	6000-7000'	54	4	0.8	0.1	-0.7	59.5	0.5
	7000-8000'	67	20	7.3	2.3	-5.0	58.6	1.5
	8000-9000'	70	44	14.7	8.7	-6.0	55.6	5.4
	9000-10,000'	68	51	18.6	13.2	-5.4	43.6	9.9
	10,000-11,000'	68	58	24.5	20.3	-4.1	29.8	8.7
	11,000-12,000'	70	62	27.0	24.1	-3.0	8.1	5.2
> 12,000'	0	60	26.5	23.5	-3.0	0.2	8.0	
Kern	5000-6000'	1	0	0.0	0.0	0.0	294.4	0.0
	6000-7000'	12	0	0.0	0.0	0.0	369.9	0.0
	7000-8000'	46	2	0.9	0.1	-0.8	336.4	0.1
	8000-9000'	72	4	7.0	0.6	-6.4	315.5	0.6
	9000-10,000'	72	24	14.1	4.4	-9.7	187.5	3.3
	10,000-11,000'	72	57	18.7	14.2	-4.5	127.9	3.9
	11,000-12,000'	76	67	23.7	21.8	-1.9	92.8	3.8
> 12,000'	2	72	26.6	25.3	-1.3	44.2	3.3	

Basin	Elevation Band	4/1/18	4/13/18	4/1/18	4/13/18	4/1 thru 4/13/18	Area Sq Mi	4/13/18
		% 4/1 Avg.	% 4/13 Avg.	SWE (in)	SWE (in)	Chg. in SWE (in)		SNODAS* (in)
Kings	5000-6000'	19	0	0.1	0.0	-0.1	101.3	0.1
	6000-7000'	54	1	1.8	0.1	-1.7	131.6	0.5
	7000-8000'	69	16	8.4	2.1	-6.2	168.6	2.5
	8000-9000'	72	44	13.8	8.3	-5.5	216.8	10.1
	9000-10,000'	71	57	17.4	13.2	-4.2	209.7	16.8
	10,000-11,000'	72	63	22.6	19.3	-3.3	189.6	13.6
	11,000-12,000'	74	69	26.7	24.6	-2.0	150.5	7.6
	> 12,000'	6	73	28.7	28.0	-0.7	51.2	5.9
Merced	5000-6000'	39	0	0.3	0.0	-0.3	70.3	0.1
	6000-7000'	59	6	4.6	0.7	-3.9	78.2	0.6
	7000-8000'	65	29	12.2	5.9	-6.3	135.0	4.0
	8000-9000'	68	47	16.9	11.9	-4.9	118.6	14.1
	9000-10,000'	69	55	21.8	17.0	-4.8	83.2	33.8
	10,000-11,000'	71	59	28.4	23.4	-4.9	37.3	30.3
	11,000-12,000'	70	66	33.2	30.4	-2.8	11.5	18.7
	> 12,000'	23	68	36.8	35.4	-1.4	1.4	15.0
Mokelumne	5000-6000'	52	2	2.3	0.2	-2.1	81.0	0.4
	6000-7000'	58	20	9.9	4.0	-5.9	63.8	2.3
	7000-8000'	63	43	17.7	13.0	-4.7	87.0	13.5
	8000-9000'	66	52	22.4	17.9	-4.4	75.4	23.0
	9000-10,000'	11	55	26.3	21.7	-4.6	7.9	28.1
Mono	6000-7000'	18	8	0.1	0.0	-0.1	378.1	0.0
	7000-8000'	57	2	0.8	0.1	-0.8	396.2	0.0
	8000-9000'	76	16	7.2	1.6	-5.5	175.3	0.4
	9000-10,000'	72	61	16.9	12.7	-4.1	63.0	7.3
	10,000-11,000'	73	74	24.7	24.7	0.0	45.8	16.1
	11,000-12,000'	74	74	27.3	27.3	0.0	25.8	12.5
	> 12,000'	0	73	28.1	27.8	-0.3	4.5	8.7
Owens	5000-6000'	0	0	0	0	0	424.2	0.0
	6000-7000'	20	0	0	0	0	412.9	0.0
	7000-8000'	50	3	1.0	0.1	-0.9	462.7	0.0
	8000-9000'	67	24	4.9	2.0	-2.9	258.5	0.5
	9000-10,000'	76	43	10.4	6.0	-4.3	190.4	2.0
	10,000-11,000'	78	61	16.2	12.4	-3.8	195.1	4.1
	11,000-12,000'	80	72	21.9	19.7	-2.2	145.5	4.7
	> 12,000'	3	77	24.7	23.4	-1.3	79.9	3.7
San Joaquin	5000-6000'	32	0	0.2	0.0	-0.2	141.0	0.0
	6000-7000'	60	1	3.8	0.1	-3.7	179.5	0.3
	7000-8000'	69	22	10.6	3.7	-7.0	211.4	1.0
	8000-9000'	71	48	16.7	10.8	-5.9	194.4	5.4
	9000-10,000'	72	61	20.6	16.8	-3.7	199.7	18.7
	10,000-11,000'	72	65	25.3	22.3	-3.0	157.9	18.5
	11,000-12,000'	75	69	28.4	26.4	-2.0	116.7	12.7
> 12,000'	24	74	29.5	28.8	-0.7	25.8	9.0	

Basin	Elevation Band	4/1/18 % 4/1 Avg.	4/13/18 % 4/13 Avg.	4/1/18 SWE (in)	4/13/18 SWE (in)	4/1 thru 4/13/18 Chg. in SWE (in)	Area Sq Mi	4/13/18 SNODAS* (in)
Stanislaus	5000-6000'	53	1	2.2	0.1	-2.1	105.5	0.4
	6000-7000'	58	21	9.9	4.0	-5.9	134.9	1.8
	7000-8000'	65	40	16.0	10.8	-5.2	142.9	10.9
	8000-9000'	68	51	21.3	16.6	-4.8	112.9	25.0
	9000-10,000'	67	57	25.9	21.4	-4.5	49.1	31.4
	10,000-11,000'	71	60	31.1	27.4	-3.6	11.8	31.6
	> 11,000'	68	63	33.5	30.8	-2.6	0.3	22.2
Tahoe	6000-7000'	65	21	7.0	2.1	-4.9	319.0	1.6
	7000-8000'	67	49	13.9	10.2	-3.7	105.7	8.2
	8000-9000'	72	55	20.3	16.3	-4.0	68.4	17.6
	9000-10,000'	75	57	24.0	18.8	-5.2	15.8	26.3
	10,000-11,000'	68	67	26.3	23.2	-3.1	0.6	25.0
Truckee	5000-6000'	68	2	2.9	0.1	-2.9	133.5	0.2
	6000-7000'	62	27	8.9	3.3	-5.5	245.4	2.7
	7000-8000'	67	51	15.3	12.3	-3.0	126.9	9.5
	8000-9000'	78	53	20.3	15.3	-5.0	39.7	21.0
	9000-10,000'	80	56	25.2	17.6	-7.6	9.4	33.8
	10,000-11,000'	0	61	27.4	20.5	-6.9	0.4	30.0
Tule	5000-6000'	6	2	0.0	0.0	0.0	51.4	0.0
	6000-7000'	42	2	0.3	0.1	-0.2	40.8	0.1
	7000-8000'	65	19	5.6	2.1	-3.5	26.7	0.1
	8000-9000'	69	35	12.7	6.1	-6.6	14.5	0.6
	9000-10,000'	64	44	16.3	10.2	-6.1	4.3	1.1
	10,000-11,000'	22	43	16.8	10.5	-6.3	0.1	0.7
Tuolumne	5000-6000'	59	1	1.6	0.0	-1.5	167.2	0.3
	6000-7000'	58	17	8.8	2.5	-6.2	139.8	4.6
	7000-8000'	62	38	14.3	9.3	-5.0	150.0	11.6
	8000-9000'	66	51	19.3	15.3	-4.1	164.1	23.6
	9000-10,000'	69	59	23.5	20.4	-3.2	173.0	32.4
	10,000-11,000'	72	64	27.2	24.7	-2.5	87.1	26.1
	11,000-12,000'	73	69	29.9	28.4	-1.5	23.9	13.8
	> 12,000'	0	70	32.0	31.0	-1.0	2.8	9.4
W. Carson	5000-6000'	41	0	0.0	0.0	0.0	24.9	0.0
	6000-7000'	63	5	2.0	0.2	-1.7	13.7	0.3
	7000-8000'	66	43	11.8	7.7	-4.1	39.2	6.7
	8000-9000'	71	56	17.3	14.1	-3.2	33.2	13.5
	9000-10,000'	72	60	21.1	17.3	-3.7	11.1	22.1
	10,000-11,000'	0	65	23.3	20.7	-2.6	1.1	25.2
W. Walker	5000-6000'	36	0	0	0	0	78.8	0.0
	6000-7000'	76	1	0.8	0.0	-0.8	68.7	0.0
	7000-8000'	73	12	7.3	0.9	-6.3	97.5	0.2
	8000-9000'	70	51	13.8	9.2	-4.6	83.6	6.7
	9000-10,000'	71	65	20.9	19.0	-1.9	73.5	21.7
	10,000-11,000'	74	66	26.0	23.8	-2.2	28.8	25.5
> 11,000'	36	67	26.3	23.6	-2.8	2.3	15.8	
Yuba	5000-6000'	50	19	6.0	3.3	-2.6	191.7	4.7
	6000-7000'	56	37	15.4	11.4	-4.0	214.6	10.5
	7000-8000'	66	50	20.4	17.9	-2.4	110.0	14.8
	8000-9000'	53	52	26.7	20.9	-5.8	3.8	25.2

* This is a comparison to the SNODAS (SNOW Data Assimilation System) nationwide product from the National Weather Service.

Location of Reports and Excel Format Tables

ftp://snowserver.colorado.edu/pub/fromLeanne/forCADWR/Near_Real_Time_Reports/

References and Additional Sources

- Guan, B., N. P. Molotch, D. E. Waliser, S. M. Jepsen, T. H. Painter, and J. Dozier. (2013). Snow water equivalent in the Sierra Nevada: Blending snow sensor observations with snowmelt model simulations. *Water Resources Research*, Vol. 49, 5029–5046, doi:10.1002/wrcr.20387.
- Painter, T.H., K. Rittger, C. McKenzie, P. Slaughter, R. E. Davis and J. Dozier. (2009) Retrieval of subpixel snow covered area, grain size, and albedo from MODIS. *Remote Sensing of the Environment*, 113: 868-879.
- Schneider D. and N.P. Molotch. (2016). Real-time estimation of snow water equivalent in the Upper Colorado River Basin using MODIS-based SWE reconstructions and SNOTEL data. *Water Resources Research*, 52(10): 7892-7910. DOI: 10.1002/2016WR019067.
- Molotch, N.P. (2009). Reconstructing snow water equivalent in the Rio Grande headwaters using remotely sensed snow cover data and a spatially distributed snowmelt model. *Hydrological Processes*, Vol. 23, doi: 10.1002/hyp.7206, 2009.
- Molotch, N.P., and S.A. Margulis. (2008) Estimating the distribution of snow water equivalent using remotely sensed snow cover data and a spatially distributed snowmelt model: a multi-resolution, multi-sensor comparison. *Advances in Water Resources*, 31, 2008.
- Molotch, N.P., and R.C. Bales. (2006). Comparison of ground-based and airborne snow-surface albedo parameterizations in an alpine watershed: impact on snowpack mass balance. *Water Resources Research*, VOL. 42, doi:10.1029/2005WR004522.
- Molotch, N.P., and R.C. Bales. (2005). Scaling snow observations from the point to the grid-element: implications for observation network design. *Water Resources Research*, VOL. 41, doi: 10.1029/2005WR004229.
- Molotch, N.P., T.H. Painter, R.C. Bales, and J. Dozier. (2004). Incorporating remotely sensed snow albedo into a spatially distributed snowmelt model. *Geophysical Research Letters*, VOL. 31, doi:10.1029/2003GL019063, 2004.